Supplementary Material

Figure S1. RT-PCR validation and overall growth of *pitpnm3*, *sars*, and *lemd3* morphants.

Table S1. Cohort demographics.

Table S2. Gene symbols and data regarding potential oligogenic inheritance.

Supplementary Methods

Supplementary Case Descriptions

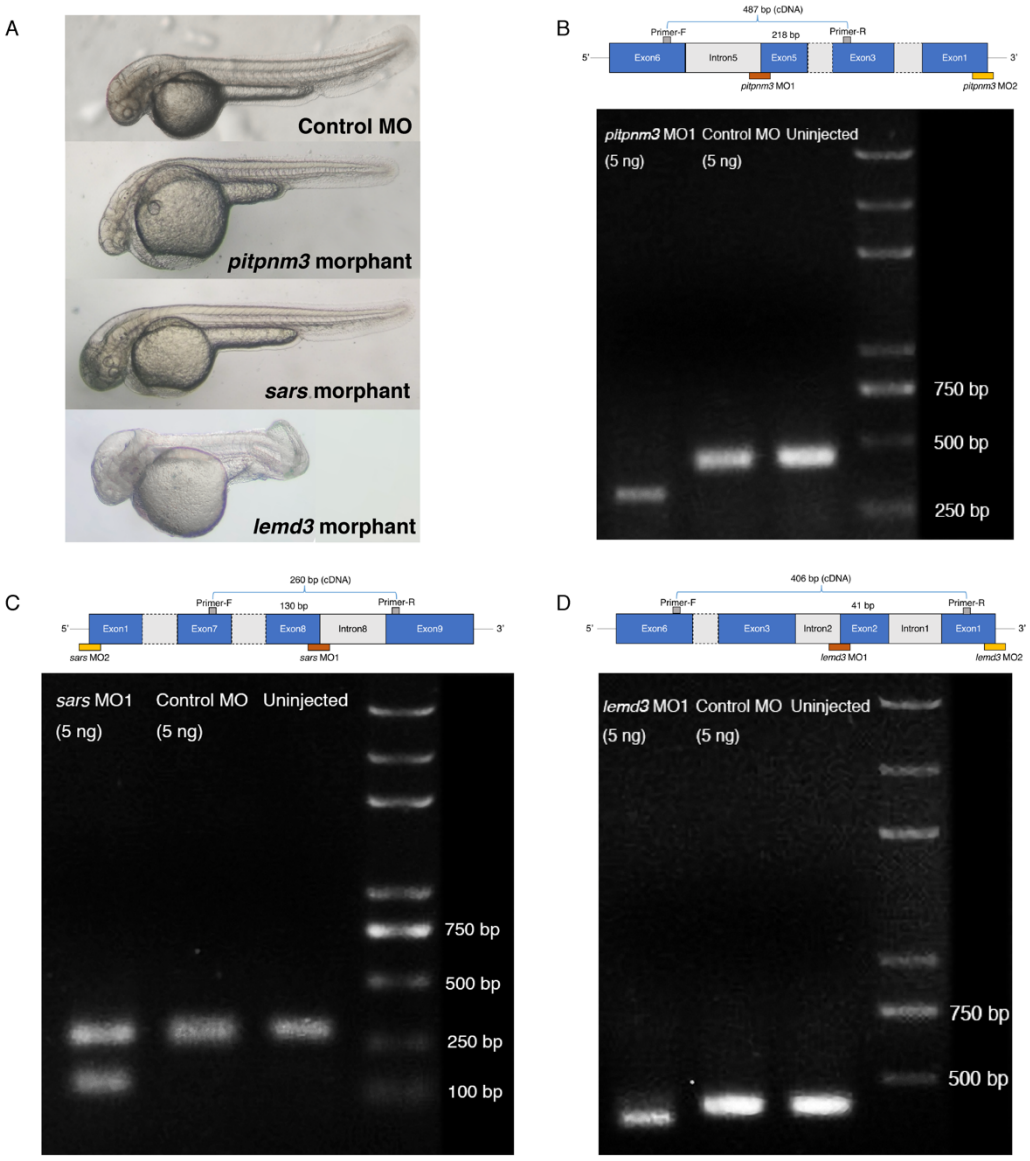

Figure S1. RT-PCR validation and overall growth of *pitpnm3*, *sars*, and *lemd3* morphants. A) Lateral view (anterior to the left) of phase microscopy images of *pitpnm3* and *sars* morphants, reveals pericardial and cranial edema, which is not detected in control embryos. Defects in the *sars* morphants were consistent with previous reports of mutants. *lemd3* morphants had disrupted axial patterning. Embryos were treated with PTU to inhibit pigment formation and render them optically clear. B-D) Diagrams indicate the target regions of MO1, MO2, and PCR primers for *pitpnm3*, *sars*, and *lemd3*. RT-PCR revealed disrupted splicing and smaller transcripts induced by injection of the splice-blocking MO (MO1) for each gene.

Table S1. Cohort demographics.

	No. of patients (%)
Total number of patients	100 (100)
Demographics	
Male, No. (%)	55 (55.0)
Mean age of diagnoses (SD), y	13.6 (6.75)
Initial presentation	
Hemorrhage, No. (%)	72 (72.0)
Seizure, No. (%)	22 (22.0)
Focal neurologic deficit, No. (%)	5 (5.0)
Asymptomatic, No. (%)	1 (1.0)
Spetzler-Martin grade	
I, No. (%)	8 (8.0)
II, No. (%)	33 (33.0)
III, No. (%)	38 (38.0)
IV, No. (%)	19 (19.0)
V, No. (%)	2 (2.0)
Associated nidal aneurysm	12 (12.0)
Hemorrhage, No. (%)	10 (10.0)
Non-hemorrhage, No. (%)	2 (2.0)

Classification of Spetzler-Martin grade was performed according to Spetzler et al [1].

Table S2. Gene symbols and data regarding potential oligogenic inheritance.

Sample ID	Inheritance	Zygosity	Chromosome	Position	Mutation type	Gene symbol	Ref transcript	Variant nomenclature	V_R/T_R	ExAC AF-East Asian	ExAC AF-total
AVM558	Maternal	Het	9	130587149	Frameshift	*ENG*	NM_000118.3	c.920dupA(p.Asn307LysfsTer27)	29/42	0	0
	de novo	Het	2	102476316	Missense	*MAP4K4*	NM_001242559.1	c.1694G>A(p.Arg565Gln)	42/97	0	0
AVM028	Paternal	Het	5	86672720	Missense	*RASA1*	NM_002890.2	c.2207A>G(p.His736Arg)	77/160	0	0
	de novo	Het	22	33253342	Missense	*TIMP3*	NM_000362.4	c.311T>C(p.Leu104Pro)	35/64	0	0
AVM359	Maternal	Het	9	130588074	Missense	*ENG*	NM_000118.3	c.589C>T(p.Arg197Trp)	18/41	0	0.000041
	de novo	Het	11	9055289	Missense	*SCUBE2*	NM_001170690.1	c.1592G>A(p.Cys531Tyr)	22/44	0	0

Abbreviations: Chr, chromosome; ExAC, Exome Aggregation Consortium; AF, allele frequency; Ref, reference; pLI, probability of loss-of-function intolerance.

Supplementary Methods

Inclusion and exclusion criteria

The diagnosis of brain arteriovenous malformation (BAVM) was confirmed by digital subtraction angiography (DSA), magnetic resonance imaging/angiography, or computed tomography angiography. The diagnosis of each patient was independently reviewed by two experienced neuroradiologists. Exclusion criteria were: 1) known diagnoses of hereditary hemorrhagic telangiectasia, capillary malformation-AVM, Sturge-Weber syndrome, or other Mendelian vascular disorders; or 2) incomplete clinical data.

Demographic information collection

We collected demographic information and clinical characteristics, including the age of diagnosis, gender, clinical symptoms at presentation, past medical history, and radiologic features of the vascular lesion. The details of the lesions, including size and clinical classifications, are shown in **Table S1**.

Variant-calling and annotation

The variant-calling and annotation were performed by the in-house developed PUMP (Peking Union Medical college hospital Pipeline). Single-nucleotide variants and internal duplications and/or deletions (aka indels) were called using the HaplotypeCaller of the Genome Analysis Toolkit, version 3.4.0. Annotated of the *de novo*, compound heterozygotes, and recessive inherited variants were calculated with Gemini (version 0.19.1) for *in silico* subtraction of parental variants from the proband's variants, with accounting for read number information extracted from BAM files. Computational prediction tools (GERP++ [2], CADD [3], SIFT [4], Polyphen-2 [5], and MutationTaster [6]) were used to predict the conservation and pathogenicity of candidate variants. All variants were compared against publicly available databases such as the 1000 Genomes Project (http://www.internationalgenome.org/), the Exome variant server, NHLBI GO Exome Sequencing Project (ESP) (http://evs.gs.washington.edu/EVS/), and the Exome Aggregation Consortium (ExAC) (http://exac.broadinstitute.org/).

Variant interpretation

Annotated variants were filtered based on an MAF <0.01. Variants related with the BAVM phenotype were prioritized based on a three-tier standard (pathogenic, likely pathogenic, VUS), taking into account variant biologic and clinical relevance as well as pathogenicity. Variant classification was performed in accordance to the ACMG guideline [7]. Variant classification was performed in accordance to the ACMG guideline. Pathogenic variants include known variants in well-established BAVM genes, and *de novo* variants with in vivo validation. Variants occurring in genes not established to be associated BAVM were classified as likely pathogenic only when it arose *de novo* or results in protein truncation in genes having common biologic activity with known BAVM candidate genes. Variants of uncertain significance were defined as 1) rare variants (MAF <0.01) in BAVM-associated genes, 2) compound heterozygous variants recurring in more than one patient, 3) compound heterozygous variants with a truncating allele, 4) homozygous variants recurring in more than one patient, and 5) *de novo* truncating variants predicted intolerable (pLI >0.9) lacking positive functional evidence.

Zebrafish husbandry and fertilization

Tg(kdrl.4:mCherry)^{pku6} transgenic zebrafish, where mCherry expression is driven by a *kdrl.4* promoter (an endothelial cell–specific gene), were used [8]. Zebrafish and embryos were maintained according to standard protocols [9]. Embryos were maintained in 0.5 g/L methylene blue to inhibit fungal contamination. 1-phenyl 2-thiourea (0.003%) was used to inhibit pigment formation.

Synthesis of human mRNA

Human *SARS*/*LEMD3* (WT and mutational type) and zebrafish *pitpnm3* ORFs were cloned into pCS2+, digested with restriction enzymes, and used as a template for *in vitro* mRNA synthesis. Extracellular transcription was performed using an Ambion mMESSAGE mMACHINE kit. mRNA (200 pg for each) was co-injected with antisense morpholinos into 1-2 cell stage zebrafish embryos.

Morpholino injection and mRNA rescue experiments

Morpholino-modified antisense oligonucleotides (GeneTools, 5 ng for each) were injected into embryos at the 1- to 2-cell stage. The *sars* MO1 (5'-AGGAGAATGTGAACAAACCTGACAC-3') targeted the exon8/intron8 splice site. The *sars* MO2 (5'- GTCTAAATCGAGCACCATTATGCCT-3') targeted the AUG initiation codon. The *lemd3* MO1 (5'- ACAGGACAGATACTTACATACTGCT-3') targeted the exon2/intron2 splice site. The *lemd3* MO2 (5'-ACGCCATCTTTGCACGAAAAACGCA-3') targeted the AUG initiation codon. The *pitpnm3* MO1 (5'- AAAGTCGCTTACTTACTTTGACACA-3') targeted the exon5/intron5 splice site. The *pitpnm3* MO2 (5'- CCCTCTGGTCTCTTTAGCCATCCTG-3') targeted the AUG initiation codon. A standard control morpholino was also used (5'-CCTCTTACCTCAGTTACAATTTATA-3'). In rescue experiments, embryos were co-injected at the 1- to 2-cell stage with wild-type/mutant human mRNA (200 pg) and splice-disrupting morpholino for each gene (MO1 at 5 ng). The mortality rate and proportion of individuals exhibiting an AVM phenotype were recorded at 48 hours post-fertilization (hpf).

Fluorescence imaging and phenotype evaluation

Zebrafish embryos at 48 hpf were fixed in 4% paraformaldehyde and embedded into 2% agarose. Fluorescence images were collected by a confocal microscopy as Z-series stacks and reconstructed as both single 2D max projection image and movies. Phenotype evaluation was performed by two experimenters in a blind fashion.

Reverse transcription-PCR

Total RNA was prepared by using Trizol from 24 hpf (for *pitpnm3* and *lemd3*) or 48 hpf (for *sars*) embryos. Total RNA was transcribed using OneScript Reverse Transcriptase kit (abm). The primers used for amplification were as follows: *pitpnm3* primers, 5’-ATGGGACACATCGACCAAACA-3’ and 5’-TTGCGACGGCATCTTGGTAG-3’; *sars* primers, 5’-TCTCCACCTGCTTCAGACAG-3’ and 5’-AAACCAAGCCTCTAAATCCAGC-3’; *lemd3* primers, 5’-TTCAGTGCCCACTACTTGTCC-3’ and 5’-CAGGGTCACCACCAATCAAC-3’

Supplementary Case Descriptions

Clinical and genetic information of BAVM patients with positive molecular findings (pathogenic variants, likely pathogenic variants, and VUS) not described in the main text. Anteroposterior and lateral DSA images confirming the diagnosis are presented for each patient.

Patient AVM028

A 4 y/o boy who suffered from headache with vomiting for 50 days, followed by 2 days of exacerbated symptoms for 2 days. Local emergent DSA revealed an AVM affecting the right parietal-occipital lobes.

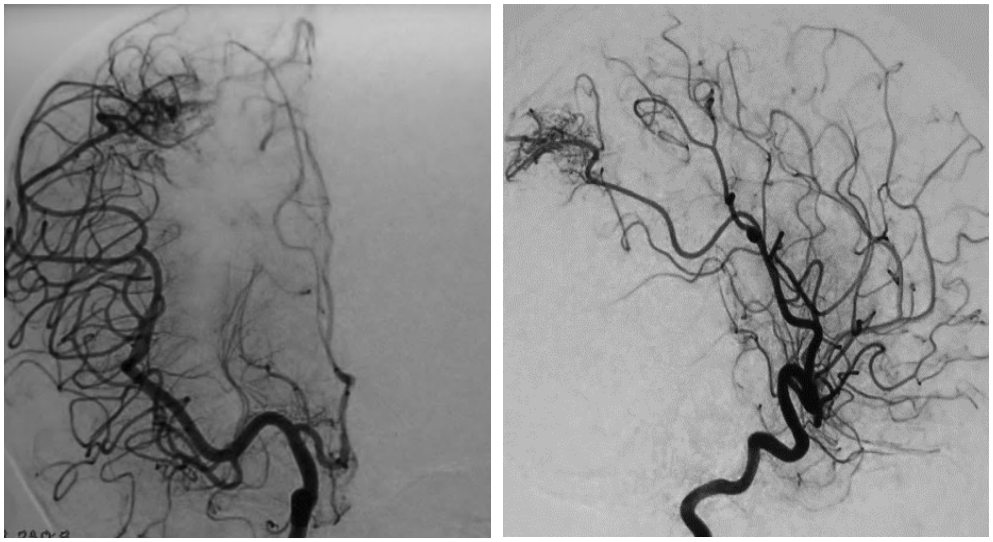

Molecular finding(s):

de novo heterozygous missense variant c.311T>C (p.Leu104Pro) in *TIMP3*, located on chr22:33253342 (**Table 1**).

Paternally inherited heterozygous missense variant c.2207A>G (p.His736Arg) in *RASA1*, located on chr5:86672720 (**Table 2**).

Patient AVM106

A 27 y/o female presenting with epilepsy for 11 years, with more-frequent seizures for the past 1 year. DSA showed a remarkable AVM lesion in the left frontal lobe.

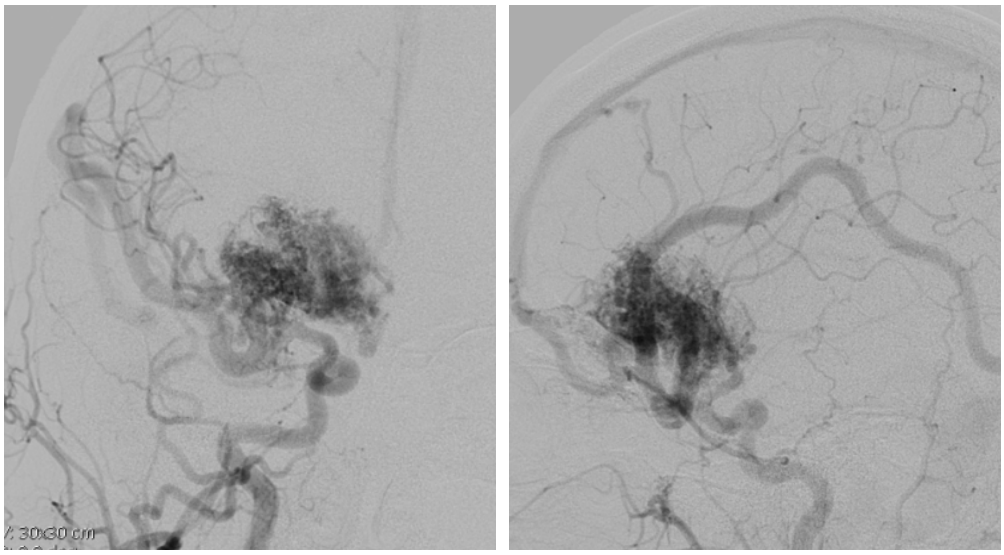

Molecular finding(s):

Maternally inherited heterozygous missense variant c.5783G>A (p.Arg1928His) in *DSCAML1*, located on chr11:117301521 (**Table 2**).

Paternally inherited heterozygous missense variant c.4574G>A (p.Arg1525His) in *DSCAML1*, located on chr11:117308649 (**Table 2**).

Patient AVM132

A 28 y/o male presenting with severe headache accompanied by nausea and vomiting. DSA showed an AVM in the area of the right basal ganglia.

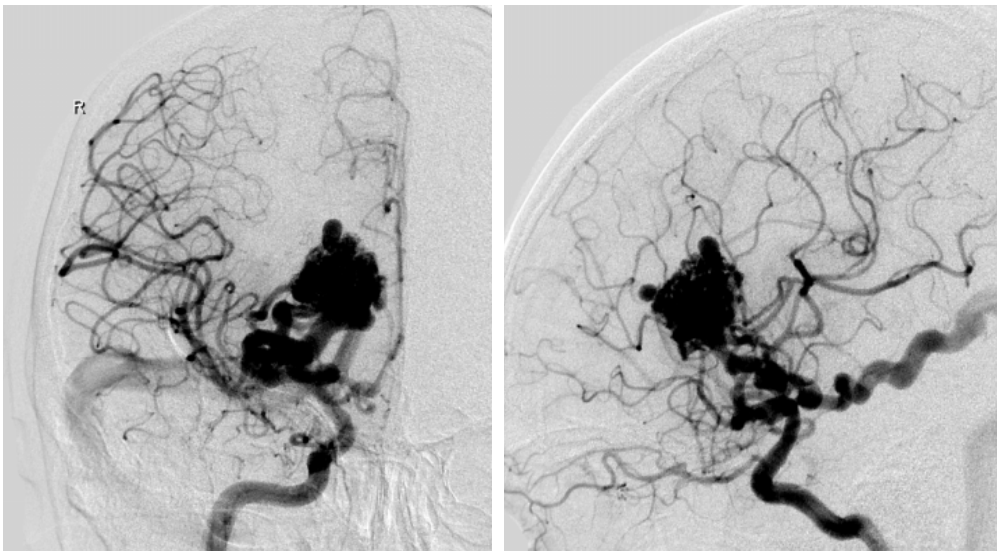

Molecular finding(s):

Paternally inherited heterozygous missense variant c.1280G>A (p.Arg427Gln) in *RASA1*, located on chr5:86649000 (**Table 2**).

Patient AVM144

A 17 y/o male who suffered from limb spasm and unconsciousness, which lasted approximately 1 minute. DSA demonstrated a left temporal AVM.

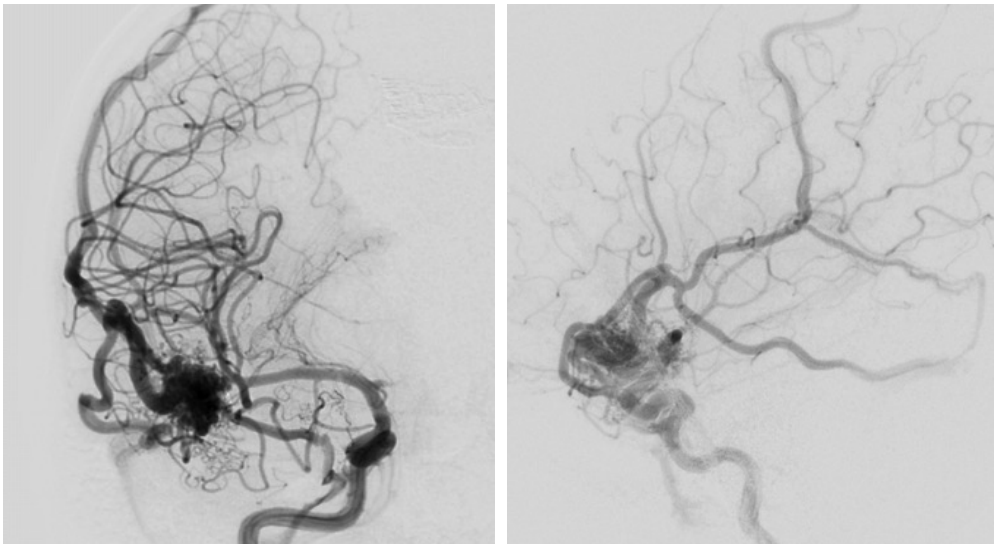

Molecular finding(s):

Paternally inherited heterozygous acceptor splicing site variant c.116-1G>A in *PTPN13*, located on chr4:87593517 (**Table 2**).

Maternally inherited heterozygous missense variant c.1000T>A (p.Ser334Thr) in PTPN13, located on chr4:87622759 (**Table 2**).

Patient AVM199

A 22 y/o female who suffered from severe headaches with vomiting for the previous 2 weeks. DSA demonstrated an AVM affecting the left fronto-parietal lobes.

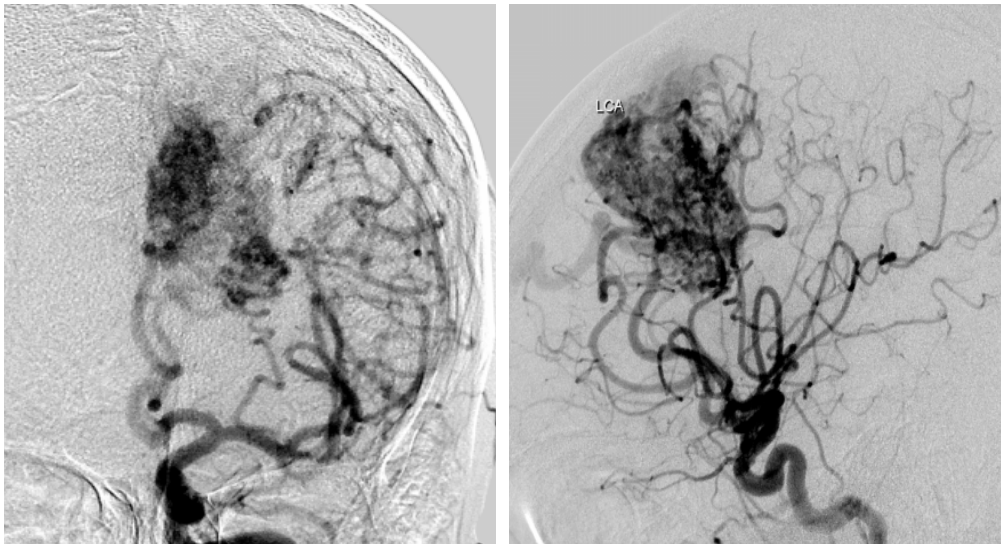

Molecular finding(s):

Paternally inherited heterozygous missense variant c.1481C>T (p.Ala494Val) in *BMPR2*, located on chr2:203417506 (**Table 2**).

Patient AVM206

A 10 y/o boy who suffered from headaches with gait instability for approximately 1 month. DSA revealed a remarkable left cerebellar hemisphere AVM.

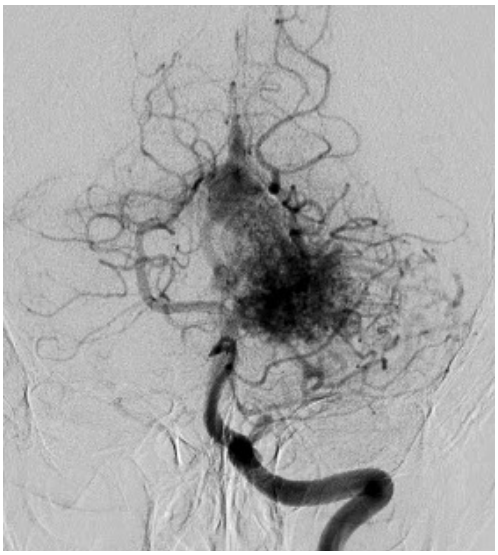
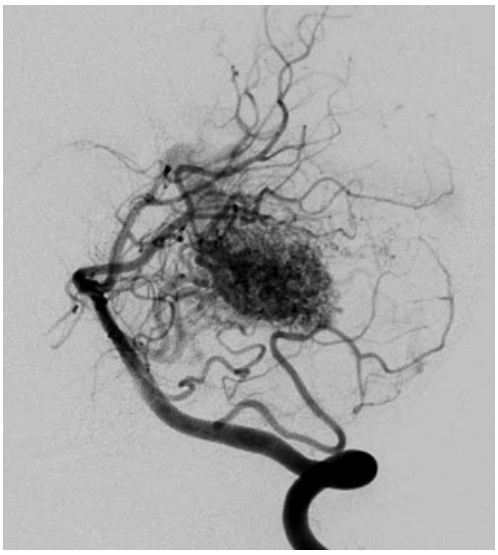

Molecular finding(s):

de novo heterozygous missense variant c.2075A>G (p.Asn692Ser) in *CDH2*, located on chr18:25565098 (**Table 1**).

Patient AVM226

A 16 y/o male who suffered from intermittent headache for 6 months. DSA displayed a BAVM, mainly in left frontal lobe.

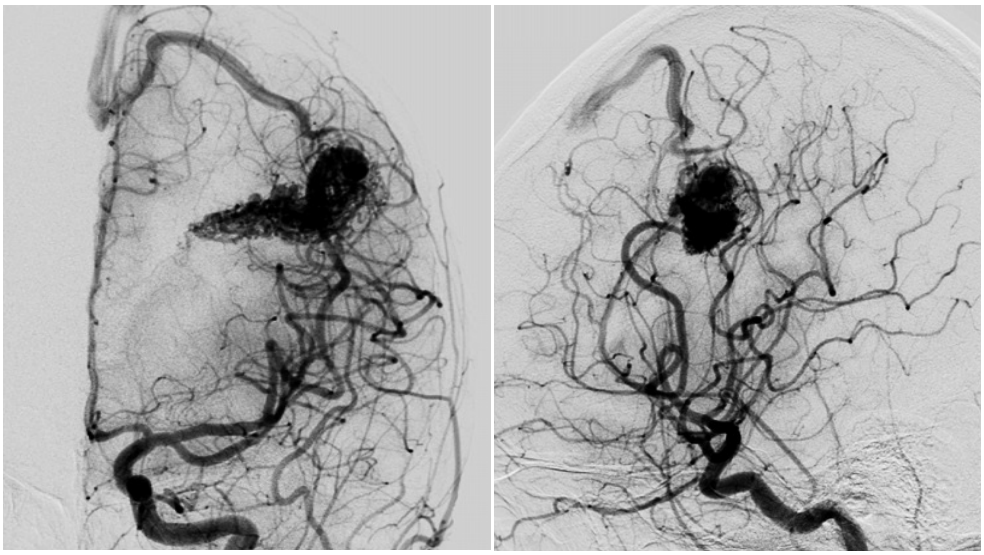

Molecular finding(s):

Maternally inherited heterozygous missense variant c.3775G>A (p.Val1259Ile) in *DSCAM*, located on chr21:41465723 (**Table 2**).

Paternally inherited heterozygous missense variant c.2966A>T (p.Gln989Leu) in *DSCAM*, located on chr21:41539197 (**Table 2**).

Patient AVM235

A 29 y/o male presenting with feeling consistent fatigue and sleepiness for 6 months. Further DSA confirmed an extensive AVM mass largely involving the right temporal lobe.

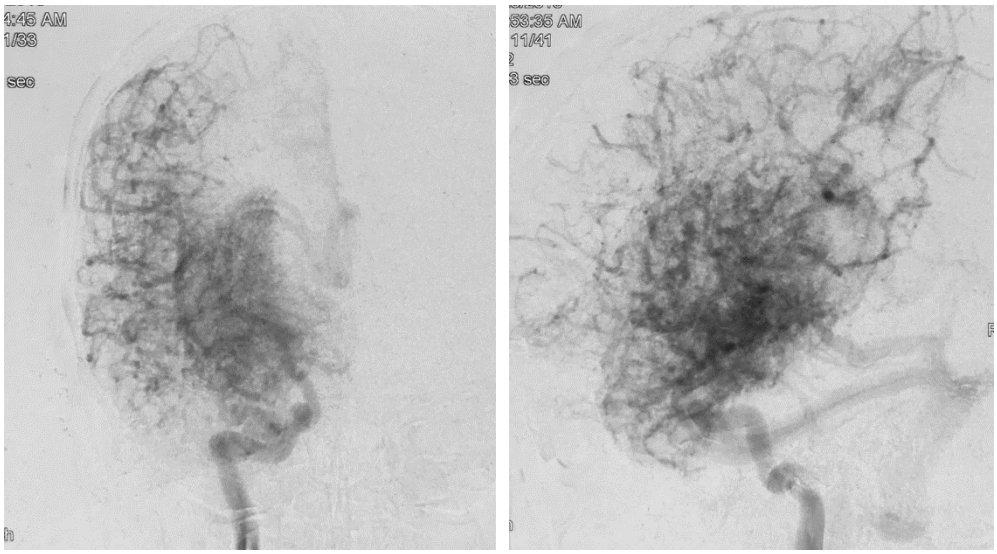

Molecular finding(s):

Paternally inherited heterozygous missense variant c.2678G>A (p.Arg893Gln) in *BMPR2*, located on chr2:203421066 (**Table 2**).

Patient AVM285

An 8 y/o girl who suffered from headache with associated vomiting for 2 weeks. DSA showed a left cerebellar hemisphere AVM.

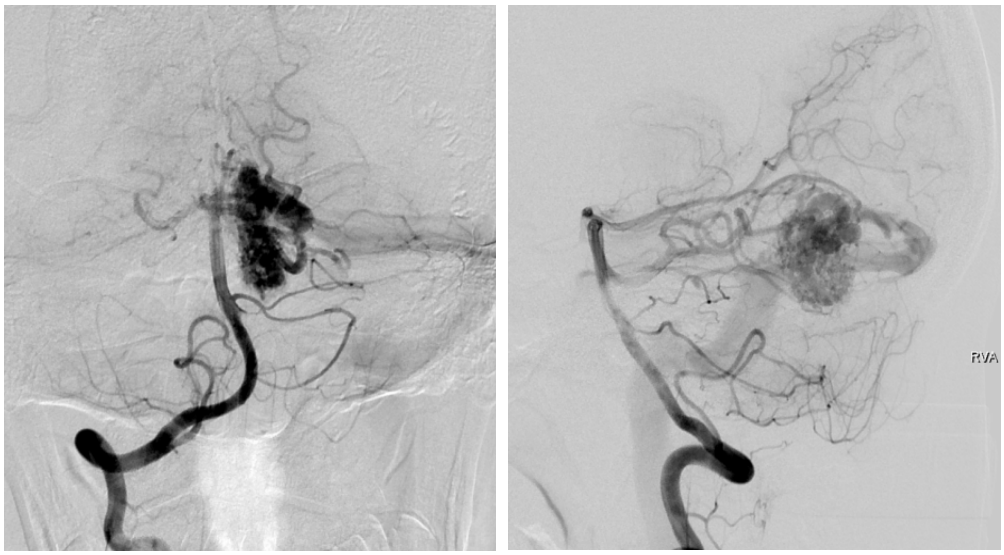

Molecular finding(s):

Paternally inherited heterozygous missense variant c.110A>G (p.Lys37Arg) in *RASA1*, located on chr5:86564378 (**Table 2**).

Maternally inherited heterozygous missense variant c.5783G>A (p.Arg1928His) in *DSCAML1*, located on chr11:117301521 (**Table 2**).

Paternally inherited heterozygous missense variant c.4574G>A (p.Arg1525His) in *DSCAML1*, located on chr11:117308649 (**Table 2**).

Patient AVM312

A 17 y/o boy who suffered from severe headache with nausea, vomiting, and loss of consciousness 20 days prior to enrollment in the study. Emergent DSA showed an AVM lesion in the medial part of the right basal ganglion.

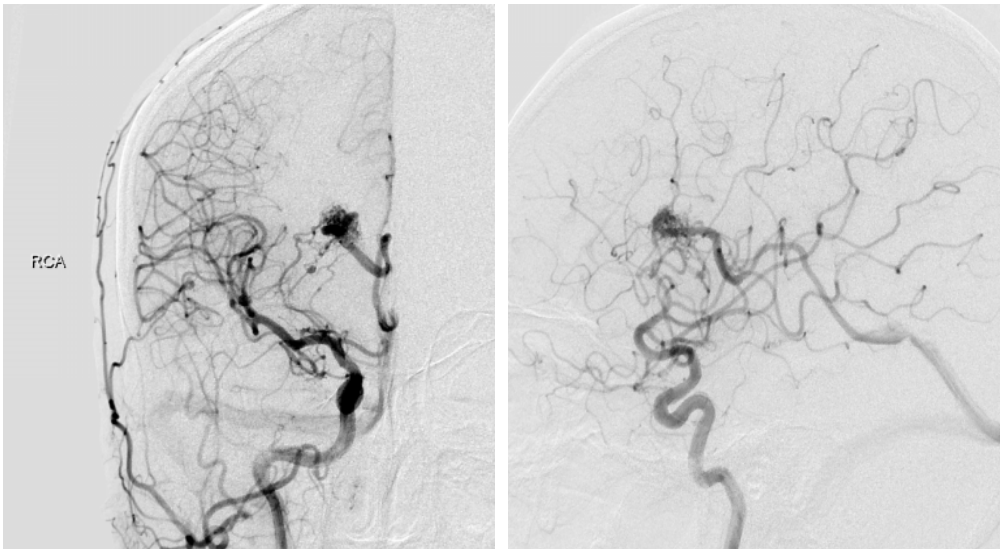

Molecular finding(s):

Paternally inherited heterozygous stop-gain variant c.1891G>T (p.Glu631Ter) in *EGFR*, located on chr7:55238010 (**Table 1**).

Patient AVM359

A 20 y/o male presenting with paroxysmal headache for 2 years, with increased severity for 2 months. DSA showed a remarkable AVM lesion, mainly located in the left occipital lobe.

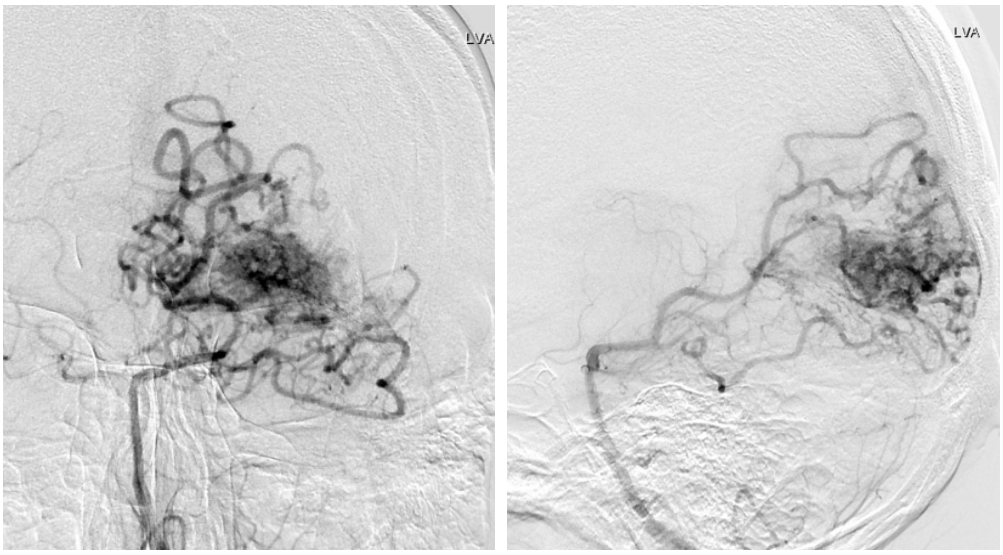

Molecular finding(s):

de novo heterozygous missense variant c.1592G>A (p.Cys531Tyr) in *SCUBE2*, located on chr11:9055289 (**Table 1**).

Maternally inherited missense variant c.589C>T (p.Arg197Trp) in *ENG*, located on chr9:130588074 (**Table 2**).

Patient AVM375

A 5 y/o boy who showed right upper- and lower-limb weakness with bradypsychia for 2 months. DSA displayed an obvious AVM severely affecting the left basal ganglion.

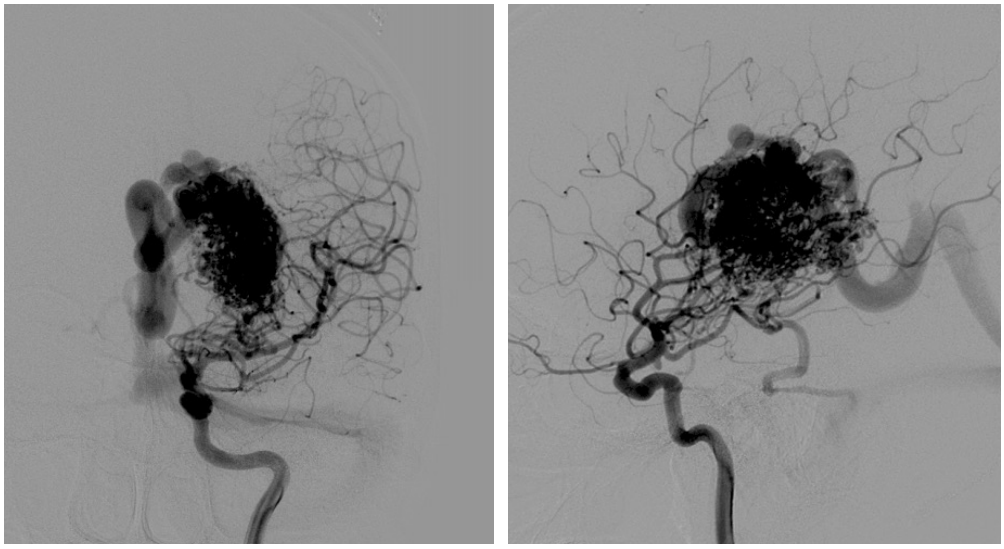

Molecular finding(s):

Maternally inherited heterozygous missense variant c.1103C>T (p.Pro368Leu) in *ACVRL1*, located on chr12:52309874 (**Table 2**).

Patient AVM401

A 16 y/o girl who suffered from seizures for 2 months. DSA showed an AVM mainly affecting the right temporal lobe.

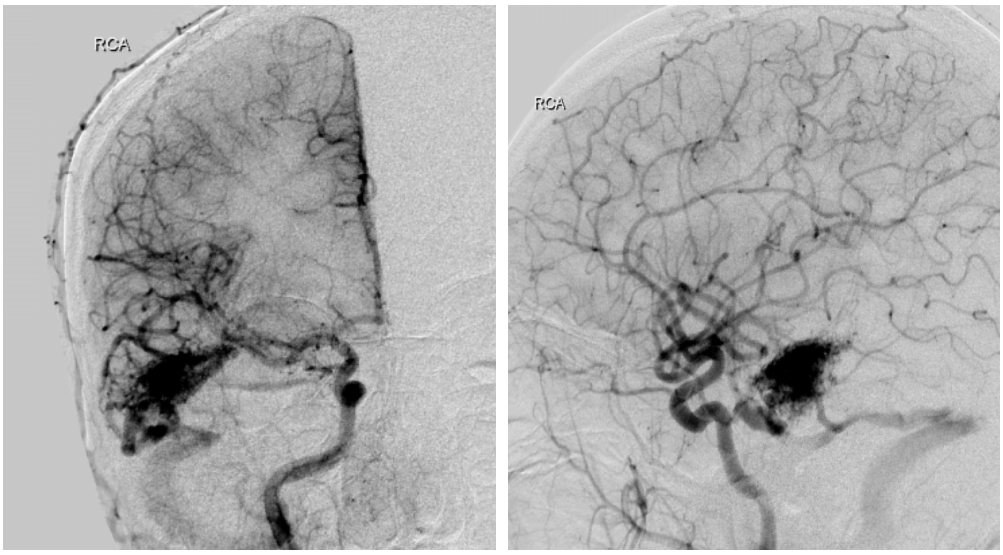

Molecular finding(s):

Paternally inherited heterozygous missense variant c.1481C>T (p.Ala494Val) in *BMPR2*, located on chr2:203417506 (**Table 2**).

Patient AVM403

A 5 y/o girl who suffered from sudden paroxysmal headaches, accompanied by right-limb weakness. DSA displayed an AVM in the left parietal lobe, functional area.

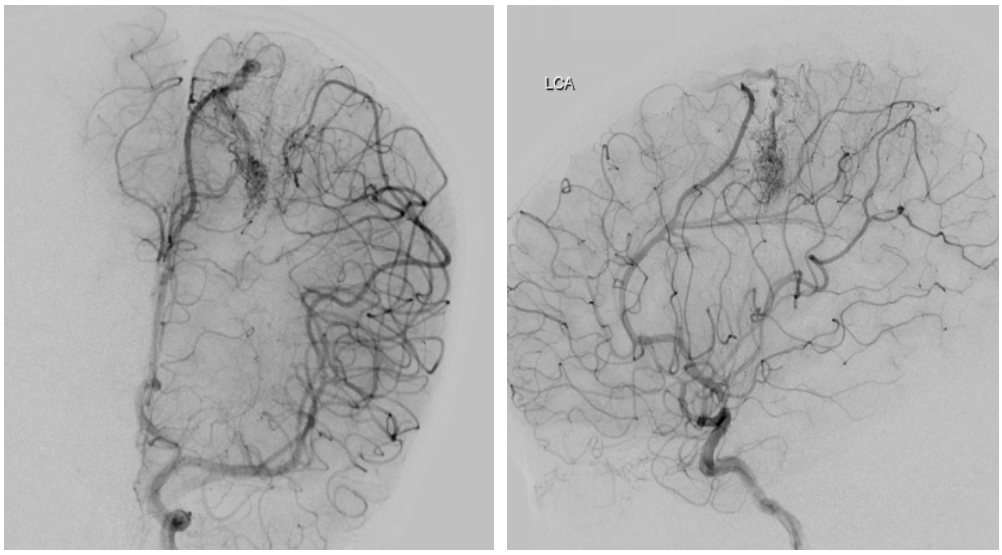

Molecular finding(s):

Maternally inherited heterozygous missense variant c.652C>T (p.Arg218Trp) in *ACVRL1*, located on chr12:52308249 (**Table 2**).

Patient AVM427

A 22 y/o male who suffered from severe headache accompanied by speech disorder for approximately 2 weeks. DSA showed an obvious AVM mass involving the left temporal and occipital lobes.

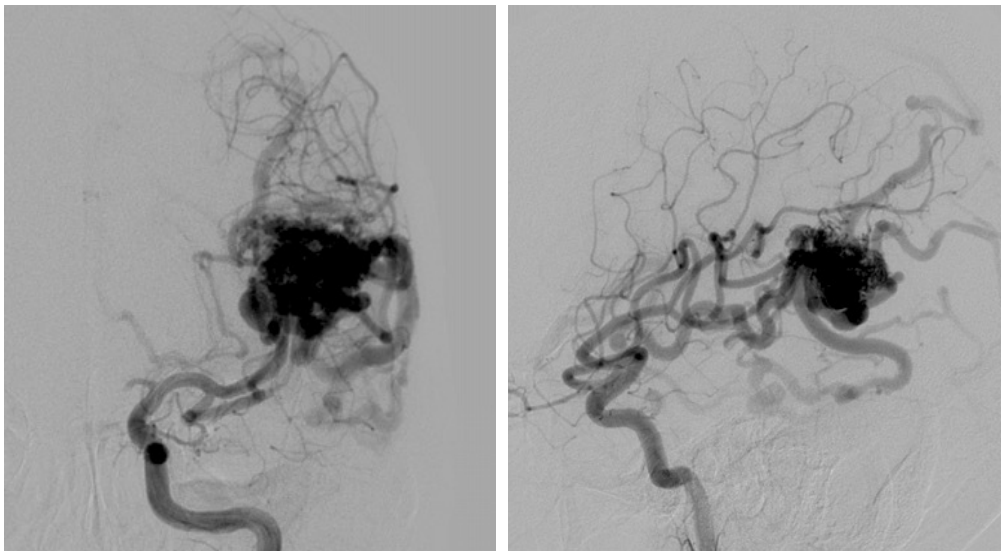

Molecular finding(s):

de novo heterozygous missense variant c.3442G>T (p.Asp1148Tyr) in *ZFYVE16*, located on chr5:79747363 (**Table 1**).

AVM457

A 20 y/o female who suffered from sudden headaches, accompanied by vomiting and loss of consciousness, lasting 2 hours. DSA showed an AVM mainly involving the right temporal and insular lobes.

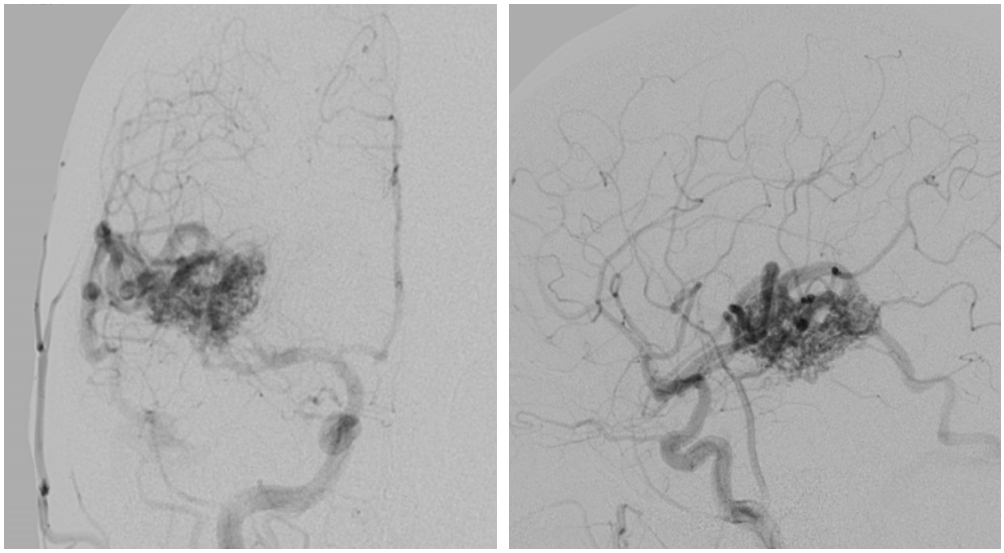

Molecular finding(s):

de novo heterozygous missense variant c.3355G>A (p.Ala1119Thr) in *PREX2*, located on chr8:69030813 (**Table 1**).

Patient AVM467

A 14 y/o boy presenting with headache without other obvious symptoms. DSA showed an AVM in right parietal lobe.

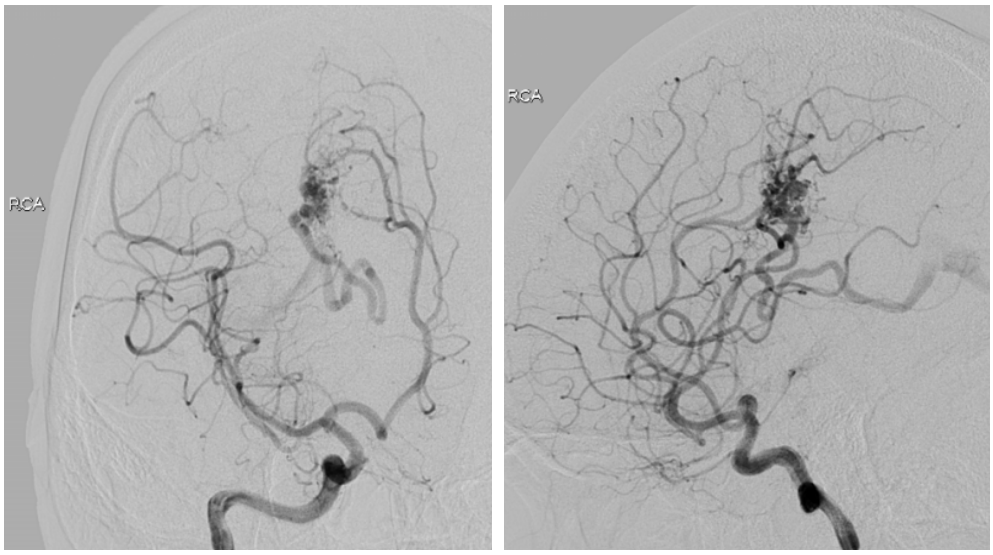

Molecular finding(s):

de novo heterozygous missense variant c.676G>A (p.Gly226Ser) in *IL17RD*, located on chr3:57139956 (**Table 1**).

Patient AVM511

A 17 y/o female who suffered from severe headaches associated with vomiting and followed by right-limb weakness. DSA demonstrated an AVM mainly located in the left basal ganglion.

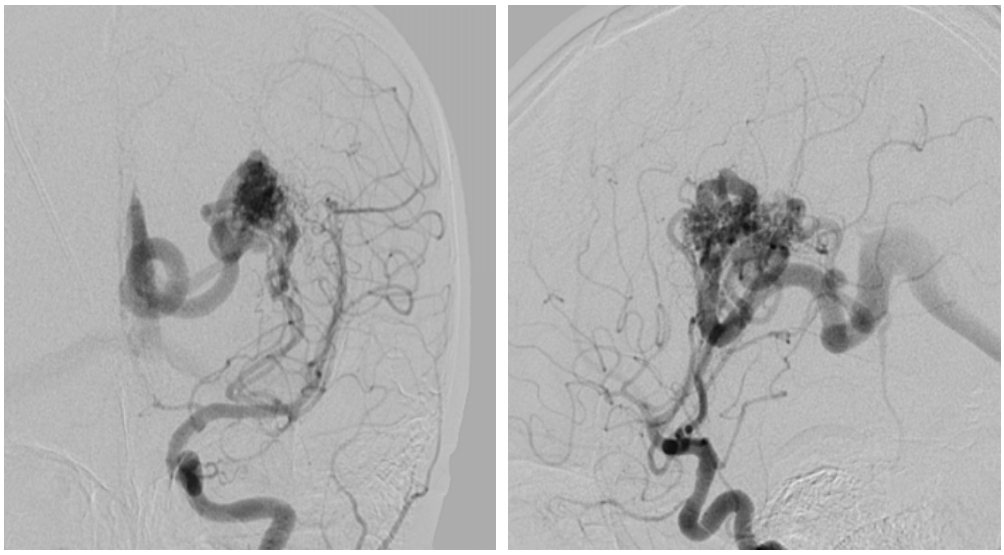

Molecular finding(s):

Maternally inherited missense variant c.1042G>A (p.Val348Ile) in *BMPR2*, located on chr2:203395591 (**Table 2**).

Patient AVM515

An 18 y/o male who suffered from severe headaches without other symptoms for the previous 10 days. DSA demonstrated an AVM mainly affecting the left basal ganglion region.

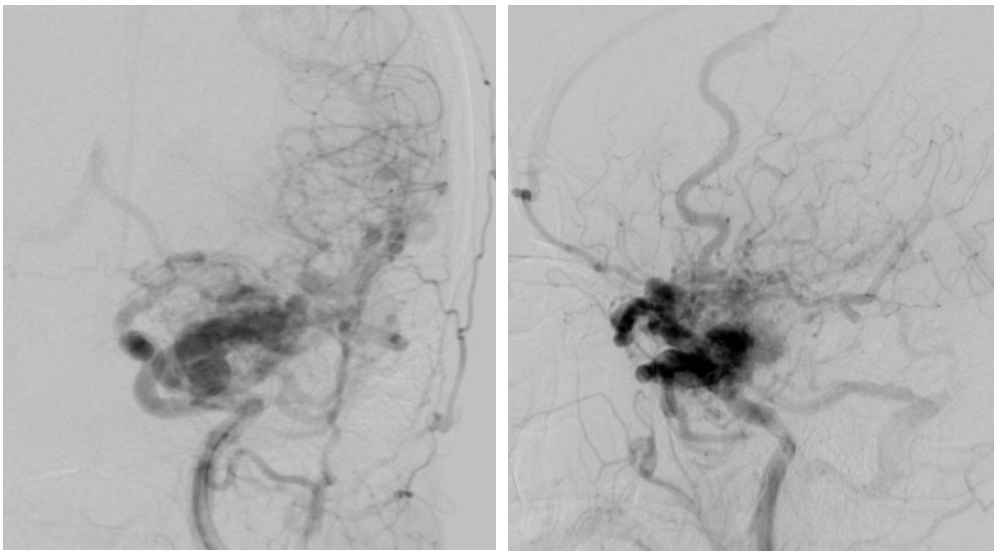

Molecular finding(s):

Paternally inherited heterozygous missense variant c.346C>T (p.Leu116Phe) in *RASA1*, located on chr5:86564614 (**Table 2**).

Patient AVM519

A 21 y/o male presenting with sudden convulsions, accompanied with limb weakness and poor balance, which lasted for 1 minute and resolved spontaneously. DSA showed an AVM mainly located in the left insular lobe region.

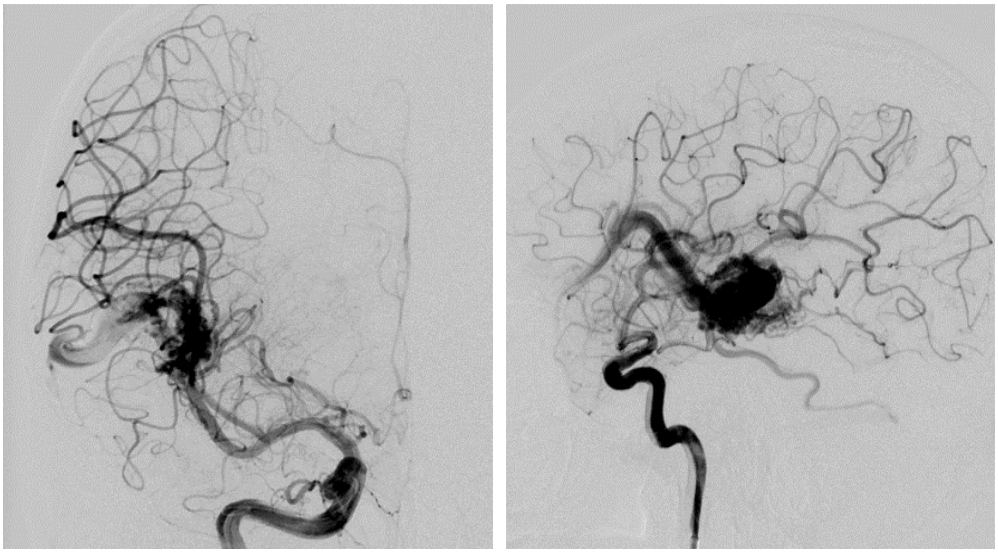

Molecular finding(s):

Paternally inherited heterozygous missense variant c.224G>C (p.Gly75Ala) in *RASA1*, located on chr5:86564492 (**Table 2**).

Patient AVM558

A 9 y/o male presenting with intermittent headaches for 4 months, associated with vomiting and nausea. DSA showed a BAVM mass largely affecting the left fronto-parietal lobes.

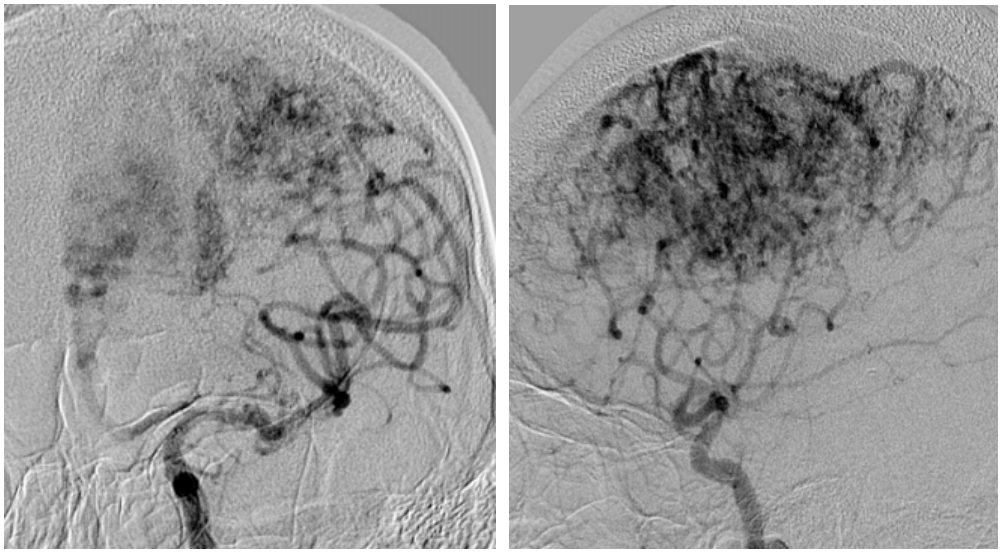

Molecular finding(s):

Maternally inherited heterozygous frameshift variant c.920dupA (p.Asn307LysfsTer27) in *ENG*, located on chr9:130587149 (**Table 1**).

de novo heterozygous missense variant c.1694G>A (p.Arg565Gln) in *MAP4K4*, located on chr2:102476316 (**Table 1**).

Patient AVM578

A 6 y/o boy presenting with paroxysmal headache, accompanied by nausea. DSA showed an AVM with venous lake located mainly in the left temporal lobe.

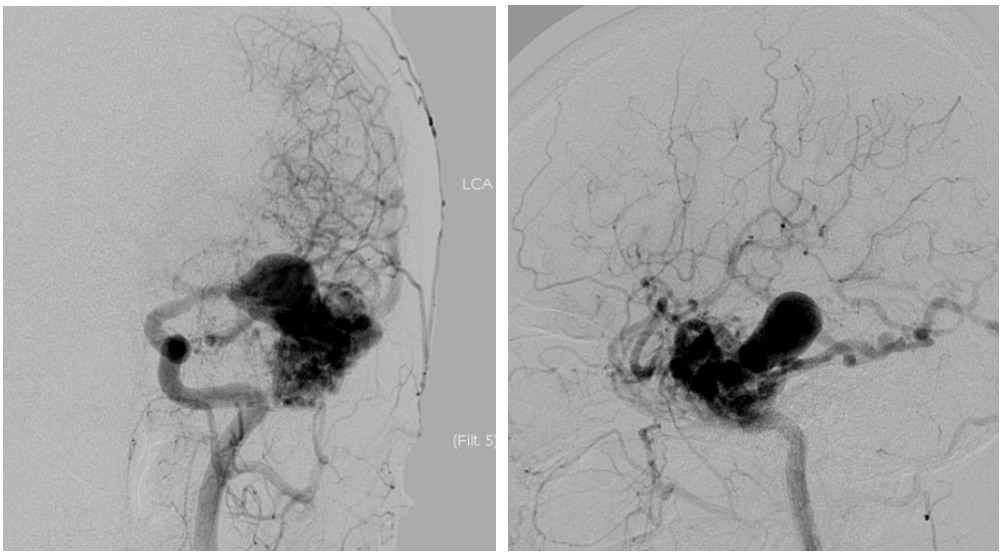

Molecular finding(s):

Paternally inherited heterozygous missense variant c.2476G>A (p.Val826Met) in *RASA1*, located on chr5:86685291 (**Table 2**).

References

1. Speizler RF, Martin NA. A proposed grading system for arteriovenous malformations. 1986. J Neurosurg 2008;**108**(1):186-93 doi: 10.3171/JNS/2008/108/01/0186.
2. Davydov EV, Goode DL, Sirota M, Cooper GM, Sidow A, Batzoglou S. Identifying a high fraction of the human genome to be under selective constraint using GERP++. PLoS Comput Biol 2010;**6**(12):e1001025 doi: 10.1371/journal.pcbi.1001025.
3. Kircher M, Witten DM, Jain P, O'Roak BJ, Cooper GM, Shendure J. A general framework for estimating the relative pathogenicity of human genetic variants. Nat Genet 2014;**46**(3):310-5 doi: 10.1038/ng.2892.
4. Vaser R, Adusumalli S, Leng SN, Sikic M, Ng PC. SIFT missense predictions for genomes. Nat Protoc 2016;**11**(1):1-9 doi: 10.1038/nprot.2015.123.
5. Adzhubei IA, Schmidt S, Peshkin L, Ramensky VE, Gerasimova A, Bork P, Kondrashov AS, Sunyaev SR. A method and server for predicting damaging missense mutations. Nat Methods 2010;**7**(4):248-9 doi: 10.1038/nmeth0410-248.
6. Schwarz JM, Cooper DN, Schuelke M, Seelow D. MutationTaster2: mutation prediction for the deep-sequencing age. Nat Methods 2014;**11**(4):361-2 doi: 10.1038/nmeth.2890.
7. Richards S, Aziz N, Bale S, Bick D, Das S, Gastier-Foster J, Grody WW, Hegde M, Lyon E, Spector E, Voelkerding K, Rehm HL, Committee ALQA. Standards and guidelines for the interpretation of sequence variants: a joint consensus recommendation of the American College of Medical Genetics and Genomics and the Association for Molecular Pathology. Genet Med 2015;**17**(5):405-24 doi: 10.1038/gim.2015.30.
8. Xia Z, Tong X, Liang F, Zhang Y, Kuok C, Zhang Y, Liu X, Zhu Z, Lin S, Zhang B. Eif3ba regulates cranial neural crest development by modulating p53 in zebrafish. Dev Biol 2013;**381**(1):83-96 doi: 10.1016/j.ydbio.2013.06.009.
9. Westerfield M. *The zebrafish book : a guide for the laboratory use of zebrafish (Danio rerio)*. Eugene, OR: Univ. of Oregon Press, 2007.